

 Open access • Book • DOI:10.1007/978-3-030-20131-9

Advances in Mechanism and Machine Science : proceedings of the 15th IFToMM World Congress on Mechanism and Machine Science — [Source link](#)

Abhilash Nayak, Stéphane Caro, Philippe Wenger

Published on: 01 Jan 2019

Topics: Revolute joint, Parallel manipulator and Workspace

Related papers:

- [Operation modes and workspace of a 4-rRUU Parallel Manipulator](#)
- [A Dual Reconfigurable 4-rRUU Parallel Manipulator](#)
- [Novel Design and Analysis of a Reconfigurable Parallel Manipulator Using Variable Geometry Approach](#)
- [QrPara: A New Reconfigurable Parallel Manipulator with 5-Axis Capability](#)
- [Workspaces associated to assembly modes of the 5r planar parallel manipulator](#)

Share this paper:    

View more about this paper here: <https://typeset.io/papers/advances-in-mechanism-and-machine-science-proceedings-of-the-34qzs9lmv6>



HAL
open science

Kinematic Analysis and Design Optimization of a 4-rRUU Parallel Manipulator

Abhilash Nayak, Stéphane Caro, Philippe Wenger

► **To cite this version:**

Abhilash Nayak, Stéphane Caro, Philippe Wenger. Kinematic Analysis and Design Optimization of a 4-rRUU Parallel Manipulator. Advances in Mechanism and Machine Science Proceedings of the 15th IFToMM World Congress on Mechanism and Machine Science, 2019, Advances in Mechanism and Machine Science Proceedings of the 15th IFToMM World Congress on Mechanism and Machine Science, 10.1007/978-3-030-20131-9 . hal-02353780

HAL Id: hal-02353780

<https://hal.archives-ouvertes.fr/hal-02353780>

Submitted on 7 Nov 2019

HAL is a multi-disciplinary open access archive for the deposit and dissemination of scientific research documents, whether they are published or not. The documents may come from teaching and research institutions in France or abroad, or from public or private research centers.

L'archive ouverte pluridisciplinaire **HAL**, est destinée au dépôt et à la diffusion de documents scientifiques de niveau recherche, publiés ou non, émanant des établissements d'enseignement et de recherche français ou étrangers, des laboratoires publics ou privés.

Kinematic Analysis and Design Optimization of a 4-rRUU Parallel Manipulator

Abhilash Nayak¹, Stéphane Caro², and Philippe Wenger²

¹ Centrale Nantes, Laboratoire des Sciences du Numérique de Nantes (LS2N),

² CNRS, Laboratoire des Sciences du Numérique de Nantes (LS2N),
{`abhilash.nayak,stephane.caro,philippe.wenger`}@ls2n.fr

Abstract. A lower-mobility parallel manipulator with multiple operation modes can be considered as inherently reconfigurable. 4-RUU parallel manipulator is one such manipulator with three different operation modes. Allowing the first revolute joint axis to have any horizontal orientation leads to a dual reconfigurable 4-rRUU mechanism. This paper presents a novel method to determine its operation modes as functions of the orientation of its base revolute joint axes. Moreover, its translational workspace is plotted for three mutually perpendicular orientations of its base revolute joint axes. With a goal to realize a working prototype, pareto optimization is used to determine its design parameters such that it has a larger singularity- and interference-free workspace while having a smaller size.

Keywords: parallel manipulator, dual reconfigurable, 4-RUU, operation modes, Pareto optimization

1 Introduction

2 Manipulator architecture

The dual reconfigurable 4-rRUUPM with a square base and a platform is shown in Fig. 1. Each limb consists of a double Hooke's joint (rR) followed by two universal joints (UU). Point L_i , $i = 1, 2, 3, 4$ lies on the pivotal axis of the double-Hooke's joint linkage. Point A_i lies on the first revolute joint axis of the PM. Points B_i and C_i are the geometric centers of the first and the second universal joints, respectively. Points L_i and C_i are the vertices of the square base and the platform, respectively. \mathcal{F}_O and \mathcal{F}_P are the coordinate frames attached to the fixed base and the moving platform such that their origins O and P lie at the centers of the respective squares. The circum-radii of the base and platform squares are denoted r_0 and r_1 , respectively. p and q are the link lengths. The revolute-joint axes vectors in i -th limb are marked \mathbf{s}_{ij} , $i = 1, 2, 3, 4$; $j = 1, \dots, 5$. Vectors \mathbf{s}_{i1} and \mathbf{s}_{i2} are always parallel, so are vectors \mathbf{s}_{i3} and \mathbf{s}_{i4} . For simplicity, it is assumed that the orientation of vector \mathbf{s}_{i1} expressed in coordinate frame \mathcal{F}_O is the same as that of \mathbf{s}_{i5} expressed in coordinate frame \mathcal{F}_P .

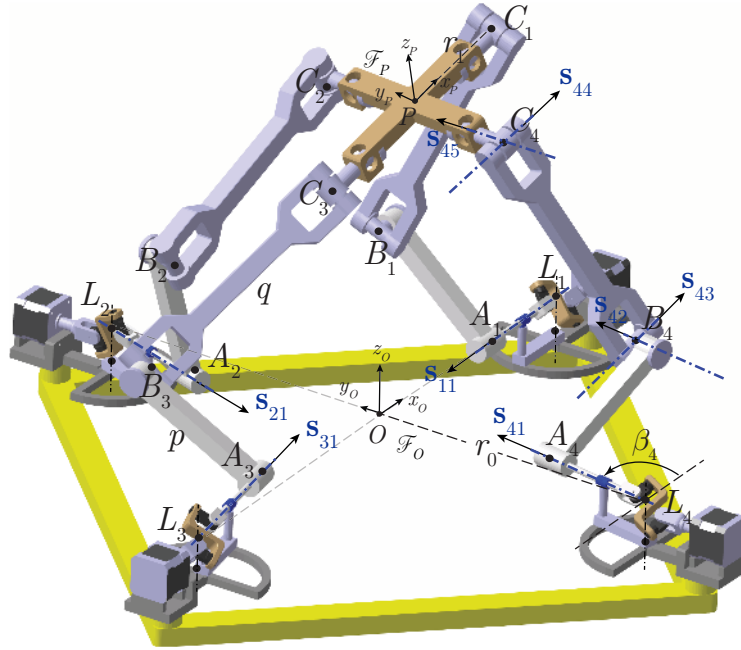


Fig. 1: A 4-rRUU parallel manipulator

3 Operation Mode Analysis

3.1 Constraint Equations

Since the reconfigurable revolute joint is actuated, a RUU limb must satisfy the following two constraints:

1. The second revolute joint axis, the fifth revolute joint axis and link BC must lie in the same plane. In other words, the scalar triple product of the corresponding vectors must be null:

$$g_i : (\mathbf{b}_i - \mathbf{c}_i)^T (\mathbf{s}_{i2} \times \mathbf{s}_{i5}) = 0, \quad i = 1, 2, 3, 4 \quad (1)$$

2. The length of link BC must be q :

$$g_{i+4} : \|\mathbf{b}_i - \mathbf{c}_i\| - q = 0, \quad i = 1, 2, 3, 4 \quad (2)$$

Since the length of link BC does not affect the operation modes of the 4-rRUU PM, only the principal geometric constraint from Eq. (1) is considered. To express it algebraically, the homogeneous coordinates of the necessary vectors ex-

pressed in frame \mathcal{F}_O are listed below:

$${}^0\mathbf{l}_i = \mathbf{R}_z(\lambda_i) [1, r_0, 0, 0]^T \quad (3a)$$

$${}^0\mathbf{a}_i = {}^0\mathbf{l}_i + \mathbf{R}_z(\lambda_i + \beta_i) [0, 0, l_i, 0]^T \quad (3b)$$

$${}^0\mathbf{b}_i = {}^0\mathbf{a}_i + \mathbf{R}_z(\lambda_i + \beta_i) [0, p \cos(\theta_i), 0, p \sin(\theta_i)]^T \quad (3c)$$

$${}^0\mathbf{c}_i = \mathbf{F} \mathbf{R}_z(\lambda_i) [1, r_1, 0, 0]^T, \quad (3d)$$

$${}^0\mathbf{s}_{i2} = \mathbf{R}_z(\lambda_i + \beta_i) [0, 0, 1, 0]^T, \quad (3e)$$

$${}^0\mathbf{s}_{i5} = \mathbf{F} \mathbf{R}_z(\lambda_i + \beta_i) [0, 0, 1, 0]^T, \quad i = 1, 2, 3, 4. \quad (3f)$$

where $l_i = |A_i L_i|$, $\mathbf{R}_z(\cdot)$ is the homogeneous rotation matrix about the z -axis, λ_i for the i -th limb is given by $\lambda_1 = 0, \lambda_2 = \frac{\pi}{2}, \lambda_3 = \pi, \lambda_4 = \frac{3\pi}{2}$ and θ_i is the actuated joint angle. \mathbf{F} is the following transformation matrix:

$$\mathbf{F} = \frac{1}{\Delta} \begin{bmatrix} \Delta & 0 & 0 & 0 \\ d_1 x_0^2 + x_1^2 - x_2^2 - x_3^2 & -2x_0x_3 + 2x_1x_2 & 2x_0x_2 + 2x_1x_3 \\ d_2 & 2x_0x_3 + 2x_1x_2 & x_0^2 - x_1^2 + x_2^2 - x_3^2 & -2x_0x_1 + 2x_2x_3 \\ d_3 & -2x_0x_2 + 2x_1x_3 & 2x_0x_1 + 2x_2x_3 & x_0^2 - x_1^2 - x_2^2 + x_3^2 \end{bmatrix} \quad (4)$$

with $\Delta = x_0^2 + x_1^2 + x_2^2 + x_3^2 \neq 0$

and $d_1 = -2x_0y_1 + 2x_1y_0 - 2x_2y_3 + 2x_3y_2$,

$d_2 = -2x_0y_2 + 2x_1y_3 + 2x_2y_0 - 2x_3y_1$,

$d_3 = -2x_0y_3 - 2x_1y_2 + 2x_2y_1 + 2x_3y_0$,

where $x_j, y_j, j = 0, 1, 2, 3$ are called *Study parameters* of the transformation \mathbf{F} . A point $P = (x_0 : x_1 : x_2 : x_3 : y_0 : y_1 : y_2 : y_3) \in \mathbb{P}^7$ represents an Euclidean transformation, if and only if P lies in a 6-dimensional quadric, $S_6^2 \in \mathbb{P}^7$ called the *Study quadric*:

$$S_6^2 : x_0y_0 + x_1y_1 + x_2y_2 + x_3y_3 = 0 \quad (5)$$

Thus, Eq. (1) is derived for each limb algebraically by substituting $t_i = \tan\left(\frac{\theta_i}{2}\right)$

and $v_i = \tan\left(\frac{\beta_i}{2}\right)$, $i = 1, 2, 3, 4$. The equations are not displayed here due to space limits.

The constraint polynomials $g_i, i = 1, 2, 3, 4$ along with Study's quadric form the following ideal³:

$$\mathcal{I} = \langle g_1, g_2, g_3, g_4, S_6^2 \rangle \subseteq k[x_0, x_1, x_2, x_3, y_0, y_1, y_2, y_3] \quad (6)$$

³ The ideal generated by the given polynomials is the set of all combinations of these polynomials using coefficients from the polynomial ring $k[x_0, x_1, x_2, x_3, y_0, y_1, y_2, y_3]$ [1].

To simplify the determination of the operation modes, the 4-rRUU PM is split into two 2-rRUU PMs [5] by considering two ideals:

$$\mathcal{I}_{(I)} = \langle g_1, g_3, \mathbb{S}_6^2 \rangle \quad (7a)$$

$$\mathcal{I}_{(II)} = \langle g_2, g_4, \mathbb{S}_6^2 \rangle \quad (7b)$$

Furthermore, $\mathcal{I}_{(I)}$ and $\mathcal{I}_{(II)}$ can be decomposed into simpler ideals using primary decomposition to understand the operation modes of the 2-rRUU PMs. Thus, the union of the corresponding prime ideals characterize the operation modes of the whole 4-rRUU PM. Two cases can be considered:

Case 1: When the revolute joint axes are arbitrarily oriented, the primary decomposition of $\mathcal{I}_{(I)}$ and $\mathcal{I}_{(II)}$ leads to one sub-ideal each. These sub-ideals depend on the design parameters and are mixed motion modes which are not of interest in the context of this paper.

Case 2: When the opposite revolute joint axes have the same orientation i.e. $v_1 = v_3$ and $v_2 = v_4$, the operation modes can be determined as follows: All planar orientations of the rR-joint axes are covered by varying $\beta_i \in [-90^\circ, 90^\circ]$ and hence $v_i \in [-1, 1]$. Design parameters were substituted as $r_0 = 2, r_1 = 3, p = 5, q = 7$ to simplify the primary decomposition of ideals $\mathcal{I}_{(I)}$ and $\mathcal{I}_{(II)}$ in Eq. (7). The operation modes could be determined only when arbitrary rational values are substituted for $v_1 = v_3 = v_{13}$ and $v_2 = v_4 = v_{24}$. The primary decomposition is performed in a computer algebra system SINGULAR and it leads to three sub-ideals each. The first two are independent of the design parameters and actuated variables. They are of the following form:

$$\begin{aligned} \mathcal{I}_{(I)} &= \mathcal{I}_{1(I)} \cap \mathcal{I}_{2(I)} \cap \mathcal{I}_{3(I)}, \\ \text{where } \mathcal{I}_{1(I)} &= \langle x_0, h_1x_1 + h_2x_2, x_1y_1 + x_2y_2 + x_3y_3 \rangle \\ \text{and } \mathcal{I}_{2(I)} &= \langle x_3, -h_2x_1 + h_1x_2, x_0y_0 + x_1y_1 + x_2y_2 \rangle \end{aligned} \quad (8a)$$

$$\begin{aligned} \mathcal{I}_{(II)} &= \mathcal{I}_{1(II)} \cap \mathcal{I}_{2(II)} \cap \mathcal{I}_{3(II)}, \\ \text{where } \mathcal{I}_{1(II)} &= \langle x_0, -h_2x_1 + h_1x_2, x_1y_1 + x_2y_2 + x_3y_3 \rangle \\ \text{and } \mathcal{I}_{2(II)} &= \langle x_3, h_1x_1 + h_2x_2, x_0y_0 + x_1y_1 + x_2y_2 \rangle \end{aligned} \quad (8b)$$

where h_1 and h_2 are functions of v_{13} and v_{24} . For instance, $\mathcal{I}_{1(I)}$ consists of

| | | | | | | | | |
|----------|----|----------------|----------------|---|---------------|---------------|---|-------------------------------|
| v_{13} | -1 | $-\frac{1}{2}$ | $-\frac{1}{4}$ | 0 | $\frac{1}{4}$ | $\frac{1}{2}$ | 1 | w |
| h_1 | -1 | -4 | -8 | 0 | 8 | 4 | 1 | $\frac{2}{w}, w \neq 0$ |
| h_2 | 0 | -3 | -15 | 0 | -15 | -3 | 0 | $1 - \frac{1}{w^2}, w \neq 0$ |

Table 1: h_1 and h_2 as functions of v_{13} such that $\langle h_1x_1 + h_2x_2 \rangle \in \mathcal{I}_{1(I)}$

x_0 and $\mathbb{S}_6^2|_{x_0=0}$ irrespective of the value of v_{13} . The remaining polynomial has

coefficients h_1 and h_2 , whose values are listed in Table 1 for arbitrarily chosen v_{13} along with their interpolated values for a general $v_{13} = w$. Thus, Eq. (8) can be further simplified as follows:

$$\begin{aligned}\mathcal{I}_{1(I)} &= \langle x_0, 2v_{13}x_1 + (v_{13}^2 - 1)x_2, x_1y_1 + x_2y_2 + x_3y_3 \rangle \\ \mathcal{I}_{2(I)} &= \langle x_3, (1 - v_{13}^2)x_1 + 2v_{13}x_2, x_0y_0 + x_1y_1 + x_2y_2 \rangle\end{aligned}\quad (9a)$$

$$\begin{aligned}\mathcal{I}_{1(II)} &= \langle x_0, (1 - v_{24}^2)x_1 + 2v_{24}x_2, x_1y_1 + x_2y_2 + x_3y_3 \rangle \\ \mathcal{I}_{2(II)} &= \langle x_3, 2v_{24}x_1 + (v_{24}^2 - 1)x_2, x_0y_0 + x_1y_1 + x_2y_2 \rangle\end{aligned}\quad (9b)$$

As a result, the first two operation modes of the 4-rRUU PM are:

$$\begin{aligned}\mathcal{I}_1 &= \mathcal{I}_{1(I)} \cup \mathcal{I}_{1(II)} \\ &= \langle x_0, 2v_{13}x_1 + (v_{13}^2 - 1)x_2, (1 - v_{24}^2)x_1 + 2v_{24}x_2, x_1y_1 + x_2y_2 + x_3y_3 \rangle\end{aligned}\quad (10a)$$

$$\begin{aligned}\mathcal{I}_2 &= \mathcal{I}_{2(I)} \cup \mathcal{I}_{2(II)} \\ &= \langle x_3, (1 - v_{13}^2)x_1 + 2v_{13}x_2, 2v_{24}x_1 + (v_{24}^2 - 1)x_2, x_0y_0 + x_1y_1 + x_2y_2 \rangle\end{aligned}\quad (10b)$$

In general, $\mathcal{I}_1 = \langle x_0, x_1, x_2, y_3 \rangle$ and $\mathcal{I}_2 = \langle x_3, x_1, x_2, y_0 \rangle$. The former corresponds to a 3-*dof* pure translational mode, where the platform is upside down with the z_P -axis pointing downwards. The latter is also a 3-*dof* translational mode, but the platform is in upright position with z_P -axis pointing upwards. An example would be the configuration (2) in [4] with $\beta_i = 90^\circ, i = 1, 2, 3, 4$.

However, the set of binomial equations $2v_{13}x_1 + (v_{13}^2 - 1)x_2 = 0$ and $(1 - v_{24}^2)x_1 + 2v_{24}x_2 = 0$ can have non-trivial values for x_1 and x_2 if the following conditions are satisfied:

$$\begin{aligned}\frac{2v_{13}}{v_{13}^2 - 1} &= \frac{1 - v_{24}^2}{2v_{24}} \implies \tan(\beta_1) = \tan(\beta_3) = -\cot(\beta_2) = -\cot(\beta_4) \\ &\implies \beta_1 = \beta_3 = \beta_2 - 90^\circ = \beta_4 - 90^\circ\end{aligned}\quad (11)$$

In that case, the first two operation modes are

$$\begin{aligned}\mathcal{I}_1 &= \mathcal{I}_{1(I)} \cup \mathcal{I}_{1(II)} \\ &= \langle x_0, 2v_{13}x_1 + (v_{13}^2 - 1)x_2, x_1y_1 + x_2y_2 + x_3y_3 \rangle\end{aligned}\quad (12a)$$

$$\begin{aligned}\mathcal{I}_2 &= \mathcal{I}_{2(I)} \cup \mathcal{I}_{2(II)} \\ &= \langle x_3, (1 - v_{13}^2)x_1 + 2v_{13}x_2, x_0y_0 + x_1y_1 + x_2y_2 \rangle.\end{aligned}\quad (12b)$$

With $x_3 = 1$, the Study parameters corresponding to the first operation mode, \mathcal{I}_1 are $[0, x_1, x_2, 1, y_0, y_1, y_2, -x_1y_1 - x_2y_2]$. Thus, only four independent parameters are sufficient to characterize this operation mode and it corresponds to a 4-*dof* Schönflies mode in which the translational motions are parametrized by y_0, y_1 and y_2 and the rotational motion is parametrized by x_1, x_2 along with $2v_{13}x_1 + (v_{13}^2 - 1)x_2 = (1 - v_{24}^2)x_1 + 2v_{24}x_2 = 0$. In this operation mode,

the platform is upside down with the z_P -axis pointing in a direction opposite to the z_O -axis. The rotational motion is about an axis located at an angle of $\beta_1 - 90^\circ = \beta_3 - 90^\circ = \beta_2 = \beta_4$ from the x_O -axis.

Similarly, with $x_0 = 1$, the Study parameters corresponding to the first operation mode, \mathcal{I}_2 are $[1, x_1, x_2, 0, -x_1y_1 - x_2y_2, y_1, y_2, y_3]$. Thus, only four independent parameters are sufficient to characterize this operation mode and it is a 4-*dof* Schönflies mode in which the translational motions are parametrized by y_1, y_2 and y_3 and the rotational motion is parametrized by x_1, x_2 along with $(1 - v_{13}^2)x_1 + 2v_{13}x_2 = 2v_{24}x_1 + (v_{24}^2 - 1)x_2 = 0$. In this operation mode, the platform is in upright position with rotational motion about an axis located at an angle of $\beta_1 - 90^\circ = \beta_3 - 90^\circ = \beta_2 = \beta_4$ from the x_O -axis.

Hence, it can be concluded from Eqs. (11) and (12) that when all the base R-joint axes of the 4-rRUU PM have the same horizontal orientations, it exhibits a Schönflies motion mode with the rotational *dof* about a horizontal axis with the same orientation as those R-joint axes. An example is the configuration (1) in [4], where $\beta_1 = \beta_3 = 90^\circ$, $\beta_2 = \beta_4 = 0^\circ$.

4 Workspace for the same orientations of base R-joint axes

The moving platform center of the 4-rRUU PM lies on the boundary of the translational workspace only when at least one of its limbs is in a fully extended or a folded configuration. In this case, the limb is said to be in a limb or serial or input singularity [3]. It can happen when the 8×4 input Jacobian matrix $\mathbf{J}_I = \frac{\partial g}{\partial t_i}$ with $i = 1, 2, 3, 4$ and $g = [g_1, g_2, \dots, g_8]$ is not full-rank. One approach to deal with the non-square matrix is to search for conditions such that all its 4×4 minors vanish as shown for a 3-RUU PM in [6]. However, the first three equations of the 3-RUU PM do not depend on the variable t_i which is the half tangent of the actuated joint variable θ_i . Likewise, here, g_i does not depend on t_i , $i = 1, 2, 3, 4$. Therefore, the input singularities corresponding to limb i can be simply calculated as $f_i : \frac{\partial g_{i+4}}{\partial t_i} = 0, i = 1, 2, 3, 4$. Eliminating t_i from f_i and g_{i+4} leads to four polynomials, S_i solely in terms of Study parameters. The singularity surfaces (tori shaped) are nothing but the varieties of these polynomials and the workspace boundary is given by their intersection. By considering the 4-rRUU PMs in Schönflies motion mode, it is possible to visualize the translational workspace boundaries for different fixed orientations of the moving platform. For instance, the singularity surfaces of a 4-rRUU PM with base R-joint axes parallel to x_O -axis and with design parameters $r_0 = 2, r_1 = 1, p = 2, q = 3$ have the

following implicit representations:

$$S_1 : x^4 + 2x^2y^2 + 2x^2z^2 + y^4 + 2y^2z^2 + z^4 - 4x^3 - 4xy^2 - 4xz^2 - 4x^2 - 24y^2 - 24z^2 + 16x + 16 = 0 \quad (13a)$$

$$S_2 : x^4 + 2x^2y^2 + 2x^2z^2 + y^4 + 2y^2z^2 + z^4 - 4x^2y - 4y^3 - 4yz^2 - 8x^2 - 20y^2 - 24z^2 + 48y = 0 \quad (13b)$$

$$S_3 : x^4 + 2x^2y^2 + 2x^2z^2 + y^4 + 2y^2z^2 + z^4 + 4x^3 + 4xy^2 + 4xz^2 - 4x^2 - 24y^2 - 24z^2 - 16x + 16 = 0 \quad (13c)$$

$$S_4 : x^4 + 2x^2y^2 + 2x^2z^2 + y^4 + 2y^2z^2 + z^4 + 4x^2y + 4y^3 + 4yz^2 - 8x^2 - 20y^2 - 24z^2 - 48y = 0 \quad (13d)$$

where the orientation of moving platform, $\phi = 0^\circ$ and (x, y, z) are the coordinates of point P . The workspace boundary for this PM is shown in Fig. 2c. Additionally, Fig. 2 shows the workspaces for three configurations of the PM with their base R-joint axes parallel to x_O, y_O and z_O -axes, henceforth named as 4-R_xUU, 4-R_yUU and 4-R_zUU PMs, respectively. The workspaces are plotted for different orientations of the moving platform including their cross-sections about a symmetric axis a for the 4-R_aUU PM, where a can be x, y or z .

5 Design optimization

With an ultimate goal to build a working prototype of the 4-rRUU PM, the design parameters are determined using a Pareto optimization procedure shown in Algorithm 1. Although there are infinitely many possible orientations of the base R-joint axes, the optimization problem is simplified by only considering 4-R_xUU, 4-R_yUU and 4-R_zUU PMs. Moreover, these PMs are examined with zero orientations of their moving platform since it is the only pose shared by them.

The design parameters are r_0, r_1, p and q . They must be homogenized to facilitate scaling of the final design, which is done by setting the circum-radius of the base, r_0 to unity. It also reduces the number of parameters and hence the computation time. Their arithmetic mean is the first objective function **ObjS**, which is an array with each of element in the range $[0, 1]$. It gives the overall size of the PM. Eventually, design parameters are varied from $l = \frac{r_0}{5}$ to $u = 2r_0$ with an increment of $d = \frac{r_0}{5}$. For a given set of $\{r_1, p, q\}$, a cube of side length $2val = 6r_0$ is discretized into $n^3 = 61^3$ points. At each of these points, the following conditions are checked in the prescribed order:

- I. *Does it belong to the workspace of the PM?*

Thanks to the polynomials $S_i(x, y, z)$ in Eq. (13) corresponding to serial singularities, a point (x, y, z) lies in the workspace when $S_i(x, y, z) < 0 \forall i \in \{1, 2, 3, 4\}$.

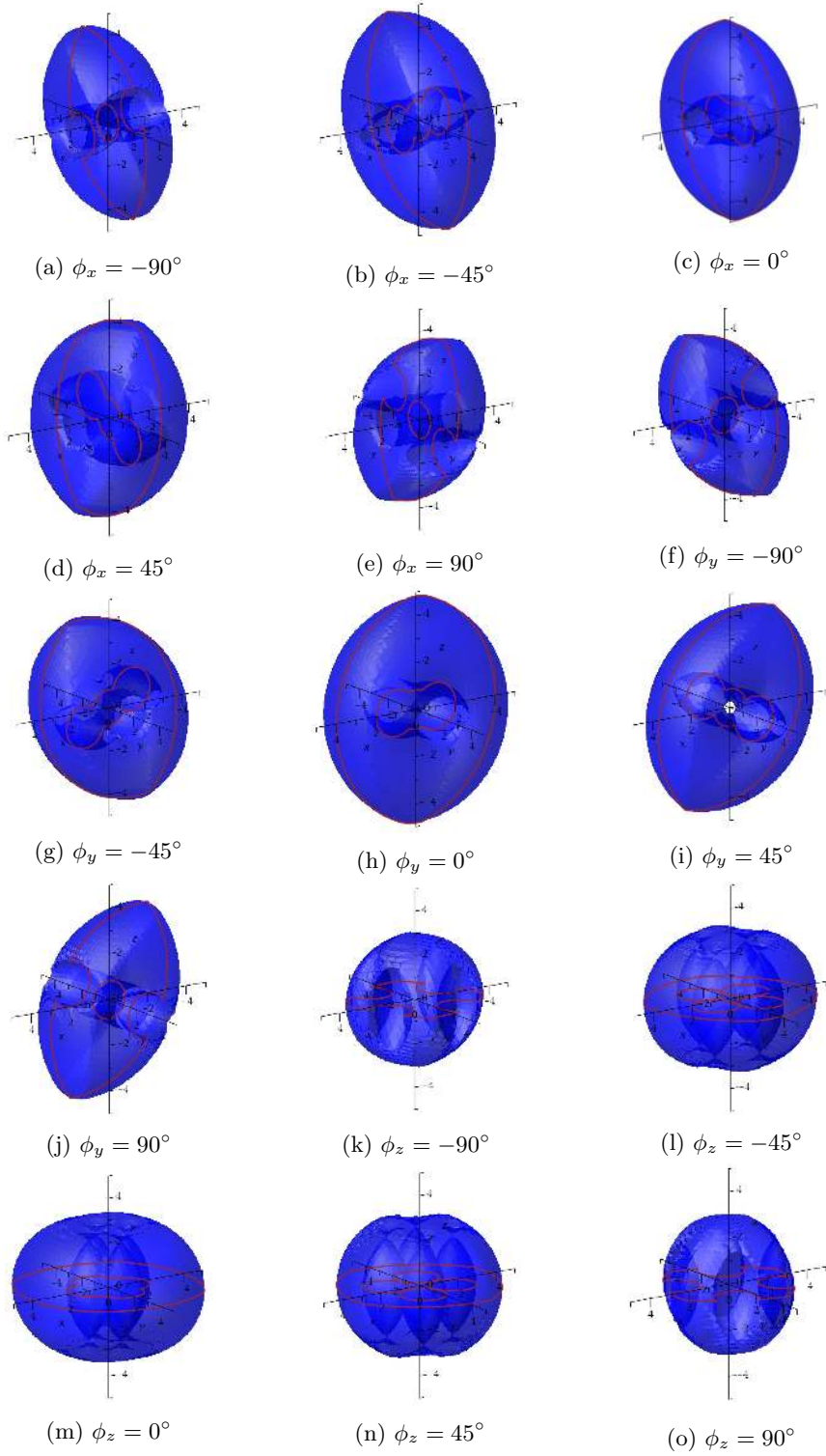


Fig. 2: Workspaces of 4- R_x UU(a-e), 4- R_y UU(f-j) and 4- R_z UU(k-o) PMs

Algorithm 1 Design optimization of a 4-rRUU PM

```

1: procedure
2:    $ax \leftarrow$  Orientation of base R-joints  $\triangleright$  1,2,3 for  $R_x$ ,  $R_y$  and  $R_z$ , respectively
3:    $\kappa \leftarrow$  Inverse condition number of the homogenized forward Jacobian matrix
4:    $\kappa_{th} \leftarrow$  Threshold value of  $\kappa$ 
5:    $r_0 \leftarrow$  Base circum-radius
6:    $r_1 \leftarrow$  Platform circum-radius
7:    $p \leftarrow$  Proximal link length
8:    $q \leftarrow$  Distal link length
9:    $\nu := 1$ 
10:   $r_0 := 1$ ;
11:  for  $r_1 \leftarrow l$  by  $d$  to  $u$  do
12:    for  $p \leftarrow l$  by  $d$  to  $u$  do
13:      for  $q \leftarrow l$  by  $d$  to  $u$  do
14:         $\text{ObjS}(\nu) := \frac{r_1 + p + q}{6}$ ;  $\triangleright$  Objective function: Size
15:         $x, y, z \leftarrow -val : res : val$ ;
16:         $n := 2 \frac{val}{res} + 1$ ;
17:        for  $i \leftarrow 1$  to  $n$  do
18:          for  $j \leftarrow 1$  to  $n$  do
19:            for  $k \leftarrow 1$  to  $n$  do
20:              if  $(x(i), y(j), z(k))$  is in the workspace and there
                exists at least one real solution to IKM without
                internal collisions with  $\kappa > \kappa_{th}$  then
21:                 $\mathbf{W}_{ax}(i, j, k) := 1$ 
22:              else
23:                 $\mathbf{W}_{ax}(i, j, k) := 0$ 
24:              end if
25:            end for
26:          end for
27:        end for
28:         $W_{ax} := \frac{\sum_i \sum_j \sum_k \mathbf{W}_{ax}(i, j, k)}{n^3}$ 
29:
30:         $\text{ObjW}(\nu) := 1 - \min_{ax=1}^3 W_{ax}$   $\triangleright$  Objective function: Workspace density
31:      end for
32:    end for
33:  end for
34:   $\nu := \nu + 1$ 
35: end procedure

```

II. *Does there exist at least one working mode?*

A working mode implies a real solution to the Inverse Kinematics Model (IKM). Given (x, y, z) , a solution to IKM involves finding the actuated joint variables. This could be done by first obtaining the coordinates of point B_i , which is the intersection of a circle with center A_i , radius p and a sphere with center C_i , radius q . In \mathbb{C}^3 , a circle and a sphere always intersect at two points. Hence, in \mathbb{R}^3 , there are at most $2^4 = 16$ IKM solutions. Thus, a real solution to IKM exists if coordinates of B_i turn out to be real.

III. *Aren't there any internal collisions?*

The links are approximated as capsules to determine their interferences. A

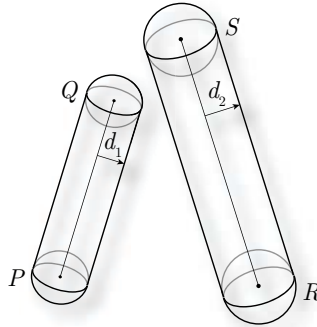


Fig. 3: Link interferences as collision between two capsules

capsule is a cylinder between two hemispheres as shown in Fig. 3. They are defined by line segments and a radius. Two capsules PQ and RS with radii d_1 and d_2 intersect if and only if the distance between line segments \overline{PQ} and \overline{RS} is less than $d_1 + d_2$. There are umpteen ways to calculate the distance between two line segments. The algorithm used here is based on the approach by Eberly [2].

Couples of eight line segments $\overline{A_i B_i}$ of length p , capsule radius $0.1p$ and $\overline{B_i C_i}$ of length q , capsule radius $0.1q$, $i = 1, 2, 3, 4$ are checked for collision. Out of these $\binom{8}{2} = 28$ combinations, there is a definite intersection between four of them sharing the point B_i . Thus, if there is an intersection between at least one of the remaining 24 couples, the PM is deemed to have internal collisions.

IV. *Is the inverse conditioning number of the forward Jacobian matrix $\kappa > \kappa_{th}$?*

Based on the theory of reciprocal screws, the reduced kinematic modeling

of the 4-rRUU PM can be expressed as

$$\mathbf{A}_r \mathbf{}^0\mathbf{t}_r = \mathbf{B}_r \dot{\theta} \implies \begin{bmatrix} (\mathbf{}^0\overrightarrow{PC}_1 \times \mathbf{}^0\mathbf{u}_1)^T & \mathbf{}^0\mathbf{u}_1^T \\ (\mathbf{}^0\overrightarrow{PC}_2 \times \mathbf{}^0\mathbf{u}_2)^T & \mathbf{}^0\mathbf{u}_2^T \\ (\mathbf{}^0\overrightarrow{PC}_3 \times \mathbf{}^0\mathbf{u}_3)^T & \mathbf{}^0\mathbf{u}_3^T \\ (\mathbf{}^0\overrightarrow{PC}_4 \times \mathbf{}^0\mathbf{u}_4)^T & \mathbf{}^0\mathbf{u}_4^T \end{bmatrix} \begin{bmatrix} \mathbf{}^0\omega \\ \mathbf{}^0\mathbf{v}_P \end{bmatrix} = \mathbf{B}_r \begin{bmatrix} \dot{\theta}_1 \\ \dot{\theta}_2 \\ \dot{\theta}_3 \\ \dot{\theta}_4 \end{bmatrix} \quad (14)$$

where $\dot{\theta}$ is the set of actuated joint rates and $\mathbf{}^0\mathbf{t}_r$ is the reduced twist of the moving platform with respect to the fixed base i.e., it contains the angular velocity vector of the moving platform and the linear velocity vector of its circum-center. Since 4-rRUU PM in its Schönflies operation mode has only one component of its angular velocity, $\mathbf{}^0\mathbf{t}_r$ is essentially a 4×1 vector. \mathbf{A}_r is the 4×4 reduced forward Jacobian matrix and it incorporates the actuation wrenches of the PM such that its columns correspond to non-zero values of $\mathbf{}^0\mathbf{t}$ with $\mathbf{}^0\mathbf{u}_i = \frac{\overrightarrow{B_iC_i}}{|\overrightarrow{B_iC_i}|}$. \mathbf{B}_r is the reduced inverse Jacobian matrix. It is diagonal with its elements being the scalar product of actuation wrenches and the actuated joint twists.

\mathbf{A}_r is homogenized by dividing its elements in the first column by r_1 since r_1 is the norm of vectors \overrightarrow{PC}_i . Thus, the inverse condition number, κ is calculated. κ gives a measure of how close the manipulator is to a parallel singularity. If it is small, the matrix is said to be ill-conditioned and is almost singular while if it is close to 1, the matrix is far from singularities. A threshold of $\kappa_{th} = 0.3$ is set and it is checked if $\kappa > \kappa_{th}$.

Consequently, the number of points satisfying conditions I-IV are counted and are divided by the total number of points considered, to obtain $W_{ax} \in [0, 1]$, where $ax = 1, 2, 3$ for 4-R_xUU, 4-R_yUU and 4-R_zUU PMs, respectively. Considering the $\min(W_1, W_2, W_3)$ leads to design parameters with larger workspaces for all three orientations of the base R-joint axes. This value is subtracted by 1 to ensure the preference of smaller values compared to larger ones in both objective functions.

Fig. 4 shows the feasible solutions, highlighting those that lie on the Pareto front. Some Pareto-optimal designs are also depicted. The Pareto-optimal design with $r_0 = 1, r_1 = 0.4, p = 1, q = 1.4$ is selected as a potential candidate for the prototype.

The goal of constructing a prototype of the 4-rRUU PM is to use it for milling operations. A milling cutter will be mounted on the moving platform, whose axis will be normal to the latter as roughly represented in Fig. 5 (not drawn to scale). The workpiece is assumed to be a cuboid of dimension $0.12 \text{ m} \times 0.05 \text{ m} \times 0.05 \text{ m}$. To place the workpiece, it is necessary choose a location in the workspace that is free of internal collisions and far from singularities and is done as follows:

The minimum condition number among 4-R_xUU, 4-R_yUU and 4-R_zUU PMs is calculated for each of their working modes. The maximum of these values is plotted in Fig. 6 throughout the translational workspace. A point F with

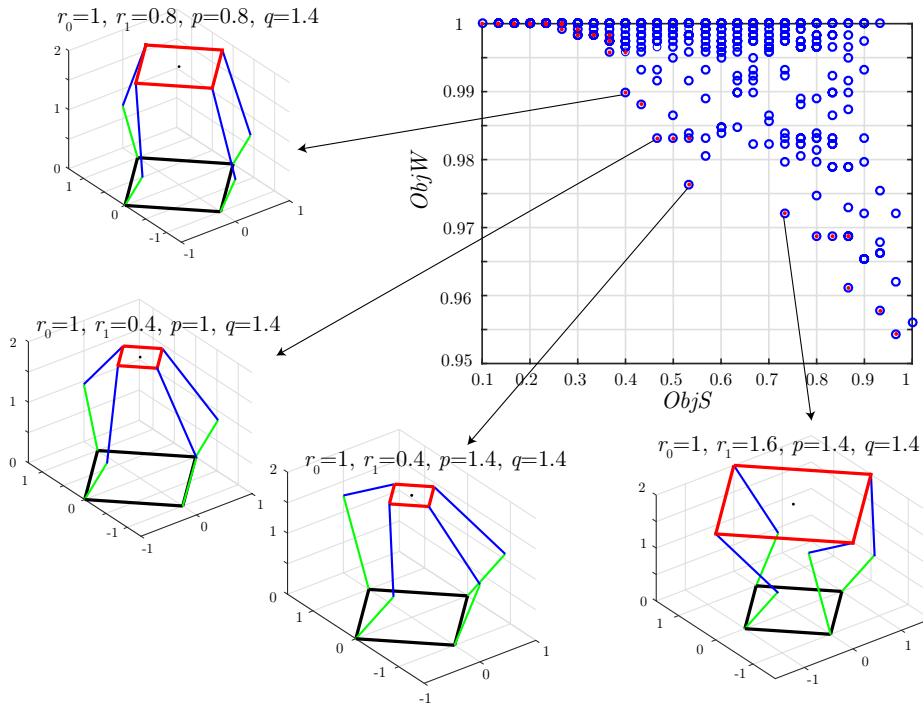


Fig. 4: Pareto-optimal solutions to the design optimization of the 4-rRUU PM.

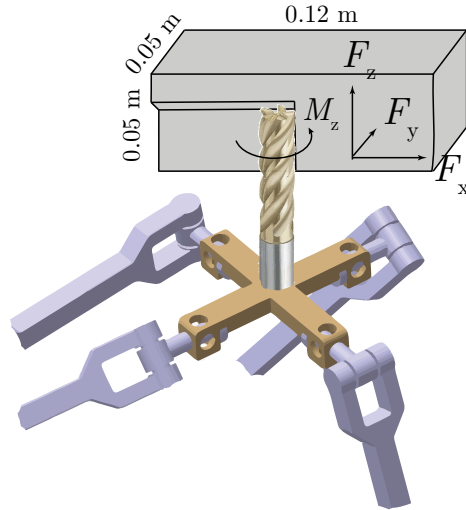


Fig. 5: Milling as a tentative application of the 4-rRUU PM prototype.

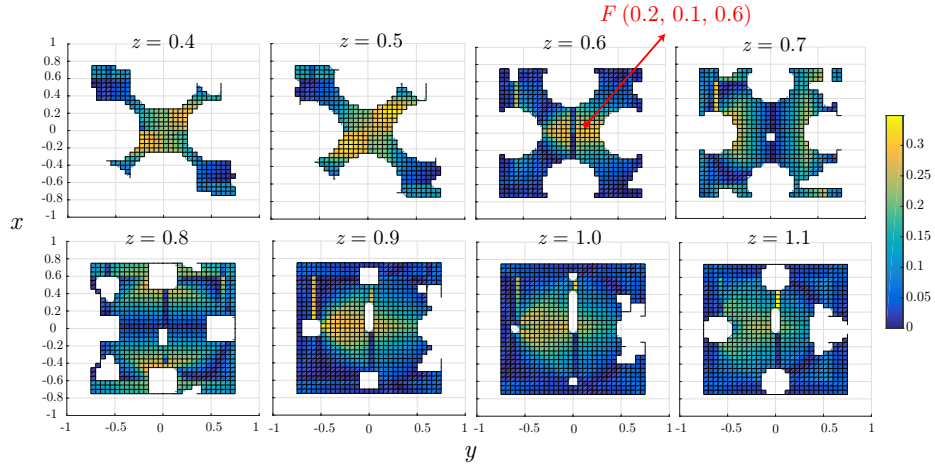


Fig. 6: Variation of condition number, $\kappa_m = \max_{ikm=1}^{16} (\min_{ax=1}^3 (\kappa))$

$x = 0.2, y = 0.1, z = 0.6$ is chosen as the midpoint of the cuboidal workpiece. Accordingly, the necessary actuated joint torques and velocities can be calculated as follows:

$$\tau = \mathbf{J}^T \mathbf{F}, \quad \dot{\theta} = (\mathbf{J}^{-1})^0 \mathbf{t}_r \quad (15)$$

$$\text{with } \mathbf{J} = \mathbf{A}_r^{-1} \mathbf{B}_r, \quad \mathbf{J}^{-1} = \mathbf{B}_r^{-1} \mathbf{A}_r, \quad (16)$$

where $\tau = [\tau_1, \tau_2, \tau_3, \tau_4]$ and $\dot{\theta} = [\dot{\theta}_1, \dot{\theta}_2, \dot{\theta}_3, \dot{\theta}_4]$ are sets of actuated joint torques and velocities, respectively. $\mathbf{F} = [M, F_x, F_y, F_z]$ and ${}^0 \mathbf{t}_r = [\omega, v_x, v_y, v_z]$ are the external forces and velocities applied on the moving platform, respectively. The direction of angular velocity ω and moment M depend on the orientation of base R-joint axes. $M_x = M_y = 0, M_z = F_x r_t$, where r_t is the tool radius. The algorithm to plot κ_m in Fig. 6 and the choice of point F ensure that there exists at least one IKM solution for each orientation of the base R-joint axes where the actuated torques and velocities are smooth.

Figure 7 shows the variation of actuated joint torques and velocities for the IKM solution with the largest κ that corresponds to Fig. 6. In this figure, the design parameters are scaled so that the fixed base of the PM is confined within a square of side 1 m. The tool radius is assumed to be 0.003 m and the remaining assigned values are listed in Table 2.

From Fig. 7, the nominal absolute torque and velocity are observed to be 10 Nm and 250 rpm, respectively. Based on these specifications, motors are bought out.

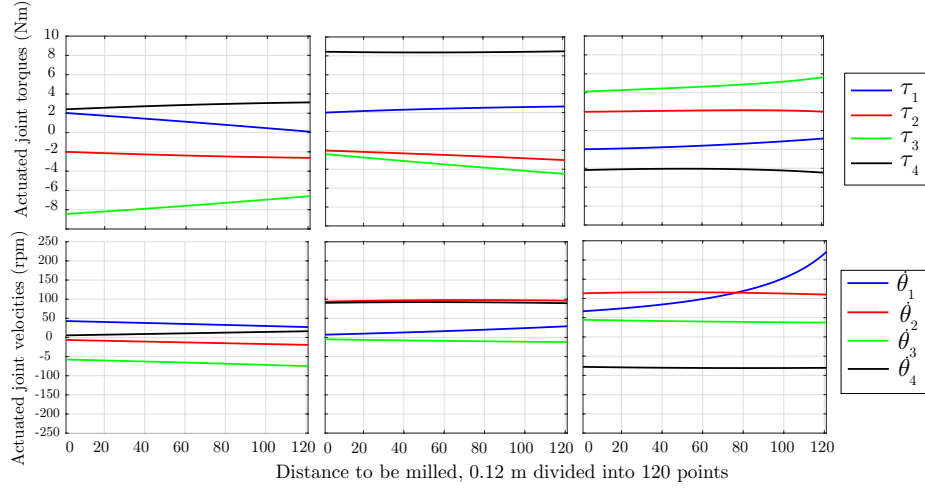


Fig. 7: Variation of actuated joint torques and velocities through 120 points divided along the distance to be milled

| | | | | |
|-----------------------------------------------|----------------------------|-----------------------|-----------------------|-----------------------|
| Design parameters (in m) | r_0 | r_1 | p | q |
| | 0.6 | 0.24 | 0.6 | 0.84 |
| External forces, \mathbf{F} | $M_z(\text{Nm})$ | $F_x(\text{N})$ | $F_y(\text{N})$ | $F_z(\text{N})$ |
| | 0.06 | 20 | 20 | 20 |
| Moving platform velocities ${}^0\mathbf{t}_r$ | $\omega(\text{rads}^{-1})$ | $v_x(\text{ms}^{-1})$ | $v_y(\text{ms}^{-1})$ | $v_z(\text{ms}^{-1})$ |
| | 0 | 0.5 | 0 | 0 |

Table 2: Inputs to calculate actuated joint torques and velocities

6 Conclusions and future work

In this paper, a dual reconfigurable 4-rRUU parallel manipulator was considered to determine its operation modes as a function of the orientation of its base revolute joint axes. The constraint equations were written down using Study's kinematic mapping for some specific base R-joint orientations such that the coefficients are always rational. It simplified the primary decomposition of the constraint equations to determine the operation modes. Furthermore, the polynomials characterizing those operation modes were interpolated to obtain the operation modes for any base R-joint orientations. Furthermore, the translational workspace was plotted for three mutually perpendicular orientations of the base R-joints, thanks to the algebraic equations describing limb singularities. With a goal to build a prototype such that the PM has the largest singularity- and collision-free translational workspace with the least size, a Pareto optimization design problem was formulated. In order to use the PM for milling applications, the necessary joint torques were calculated based on which, the motors, controller board and components to be manufactured are bought out. As a part of the future work, the working prototype of the analyzed PM will be realized.

References

1. Cox, D.A., Little, J., O'Shea, D.: Ideals, Varieties, and Algorithms: An Introduction to Computational Algebraic Geometry and Commutative Algebra, 3rd edn. Springer (2007)
2. Eberly, D.H.: Chapter 15 - intersection methods. In: D.H. Eberly (ed.) 3D Game Engine Design (Second Edition), The Morgan Kaufmann Series in Interactive 3D Technology, second edition edn., pp. 681 – 717. Morgan Kaufmann, San Francisco (2007)
3. Gosselin, C., Angeles, J.: Singularity analysis of closed-loop kinematic chains. *IEEE Transactions on Robotics and Automation* **6**(3), 281–290 (1990)
4. Nayak, A., Caro, S., Wenger, P.: A Dual Reconfigurable 4-rRUU Parallel Manipulator. In: The 4th IEEE/IFToMM International conference on Reconfigurable Mechanisms and Robots (ReMAR2018). Delft, Netherlands (2018)
5. Nurahmi, L., Caro, S., Wenger, P., Schadlbauer, J., Husty, M.: Reconfiguration analysis of a 4-ruu parallel manipulator. *Mechanism and Machine Theory* **96**, 269–289 (2016)
6. Stigger, T., Pfurner, M., Husty, M.: Workspace and singularity analysis of a 3-ruu parallel manipulator. In: B. Corves, P. Wenger, M. Hüsing (eds.) *EuCoMeS 2018*, pp. 325–332. Springer International Publishing, Cham (2019)